Science Advances

AAAS

advances.sciencemag.org/cgi/content/full/2/10/e1600873/DC1

Supplementary Materials for

Relative impacts of mitigation, temperature, and precipitation on 21st-century megadrought risk in the American Southwest

Toby R. Ault, Justin S. Mankin, Benjamin I. Cook, Jason E. Smerdon

Published 5 October 2016, *Sci. Adv.* **2**, e1600873 (2016)
DOI: 10.1126/sciadv.1600873

This PDF file includes:

Relative impacts of mitigation, temperature, and rainfall on 21st-century megadrought risk in the American Southwest.

Toby R. Ault, Justin S. Mankin, Ben I. Cook, and Jason E. Smerdon

September 27, 2016

1 Supplementary Material

This document presents several additional pieces of information supporting our overarching arguments that: (1) megadrought risk changes as a function of "mean state" and temperature; and (2) most models in the CMIP5 archive do not simulate sufficient precipitation change to overcome the effect warming will have on regional moisture balance. Specifically, Figure S1 provides additional information about the models used in Figure 1 of the main text by supplying model names. Similarly, Figure S2 shows the full range of all variables in all models plotted in Figure 1c of the main text. Figure S3 confirms that the seasonality of the precipitation and temperature anomalies do not fundamentally alter the characteristics of the PDF in Figure 2. Instead, it supports our argument that temperature plays a major role in shaping future megadrought risk. The following section (along with Figures S4 and S5) presents an analytical check on the Monte Carlo PDF generated for Figure 1.

Finally, temporal autocorrelation is a source of uncertainty not factored in to the 2D PDF in Figure 1. To address the role it could play in altering this PDF, we have computed megadrought risk using different models of persistence (Figure S6). We consider both lag-1 autocorrelation (AR(1)) and power-law distributions instead of white noise *(8)*. The autocorrelation parameter used in this case was 0.2 (corresponding to an e-folding time of about seven months) and the power law scaling coefficient was 0.5. Both of these values are supported by observations of autocorrelation on interannual timescales, as discussed in *(8)*, and references therein. In both cases, risks of

megadrought increase in the high gradient (gray) area of Figure 1, where values are already between 0.1 and 0.8. Higher values for the autocorrelation or power law coefficients would heighten risks even further in the same region. Accordingly, the results shown in Figure 1 are to be regarded as slightly conservative estimates of true risk because autocorrelation/persistence would cause values to increase in the high-gradient areas (as also argued by *(8)*). We have nevertheless elected to use the white noise based 2D PDF in Figure 1 because it is more appropriate for evaluating precipitation alongside drought indicators that exhibit varying degrees of autocorrelation.

1.1 Analytical PDF of megadrought

Analytically estimating the 2D PDF of prolonged drought risk as a function of changes in the mean ($\Delta\mu$) and standard deviation ($\epsilon\sigma'$) requires us to describe both: (a) the reduction in variance of $X_w(t)$ as a function of smoothing window length (w) for a given pair of values for $\Delta\mu$ and $\delta\sigma$; and (b) the probability of non-mutually exclusive megadrought "events."

Because X_w is a simple moving average (MA) time series, it is straightforward to derive an expression for its variance:

$$\mathrm{Var[X_w]} =< \mathrm{X_w^T X_w} >= \left(\frac{1}{\mathrm{w}}\mathrm{z'_t} + \frac{1}{\mathrm{w}}\mathrm{z'_{t-1}} + \frac{1}{\mathrm{w}}\mathrm{z'_{t-2}} + \ldots + \frac{1}{\mathrm{w}}\mathrm{z'_{t-w}}\right)^2. \tag{S1}$$

If z'_t is assumed to be "white" in time, then all of the lag covariances of z'_t above will be equal to zero ($\mathrm{Cov[z'_{t-i}, z'_{t-j}]} = 0$, for $i \neq j$), and all of the zero lag covariance terms above will simply be the variance of z'_t ($\mathrm{Cov[z'_{t-n}, z'_{t-n}]} = \sigma_z^2$, for $n = 0, 1, \ldots, w$). Equation S1 therefore simplifies to:

$$\mathrm{Var[X_w]} = \left(\frac{1}{\mathrm{w}^2}\sigma_\mathrm{z}^2 + \frac{1}{\mathrm{w}^2}\sigma_\mathrm{z}^2 + ... + \frac{1}{\mathrm{w}^2}\sigma_\mathrm{z}^2\right) = \sum_{\mathrm{i}=1}^{\mathrm{w}} \frac{1}{\mathrm{w}^2}\sigma_\mathrm{z}^2 = \mathrm{w}\left(\frac{1}{\mathrm{w}^2}\sigma_\mathrm{z}^2\right) = \frac{1}{\mathrm{w}}\sigma_\mathrm{z}^2 \tag{S2}$$

If z'_t has unit standard deviation and a mean of zero, then the variance of X_w as a function of w is simply $\frac{1}{w}$, which is shown in Figure S4 for a very wide range of averaging windows and compared with direct estimates of variances of smoothed Monte Carlo realizations.

With the above analytical expression for the variance of X_w, we estimate the probability that *at least one* megadrought event occurs over a given time period. Recall that if the probabilities of two independent events (A and B) are known, then the probability of at least one of these events occurring ($\Pr(A \cup B)$) is simply $\Pr(A) + \Pr(B) - \Pr(A \cap B)$.

Again, if the underlying distribution of z'_t is white, then over a finite period of time (of duration N) there are N/w degrees of freedom in the smoothed time series X_w. Letting $\Pr(A_i)$ denote the probability of a single value of the time series X_w falling at or below q (i.e., the probability of a megadrought event), then we are interested in the probability:

$$\Pr(A_1 \cup A_2 \cup \ldots \cup A_n) = \sum_{i=1}^{N/w} \Pr(A_i) - \prod_{i=1}^{N/w} \Pr(A_i). \tag{S3}$$

Note that $\Pr(A_1) = \Pr(A_2) = \Pr(A_n)$, so that equation $S3$ can be simplified as $(N/w)\Pr(A) - \Pr(A)^{N/w}$.

Finally, the distribution of X_w will be Gaussian with mean $\Delta\mu$ and standard deviation $\frac{1}{\sqrt{w}}\delta\sigma$ because this time series is generated from averaging z'_t, which itself is normally distributed. The probability of a single element in X_w attaining a value equal to a given threshold (q) is therefore the probability density function of the normal distribution with mean $\Delta\mu$ and $\frac{1}{\sqrt{w}}\delta\sigma_z$ standard deviation:

$$\Pr\left(q|\Delta\mu, \frac{\delta\sigma_z}{\sqrt{w}}\right) = \frac{\sqrt{w}}{\delta\sigma_z\sqrt{2\pi}} \exp\left(-\frac{w(q-\Delta\mu)^2}{2(\delta\sigma)^2}\right), \tag{S4}$$

and the probability of X_w reaching a value equal to or below q is the cumulative density function of equation S4 evaluated for a given q.

2 Figures

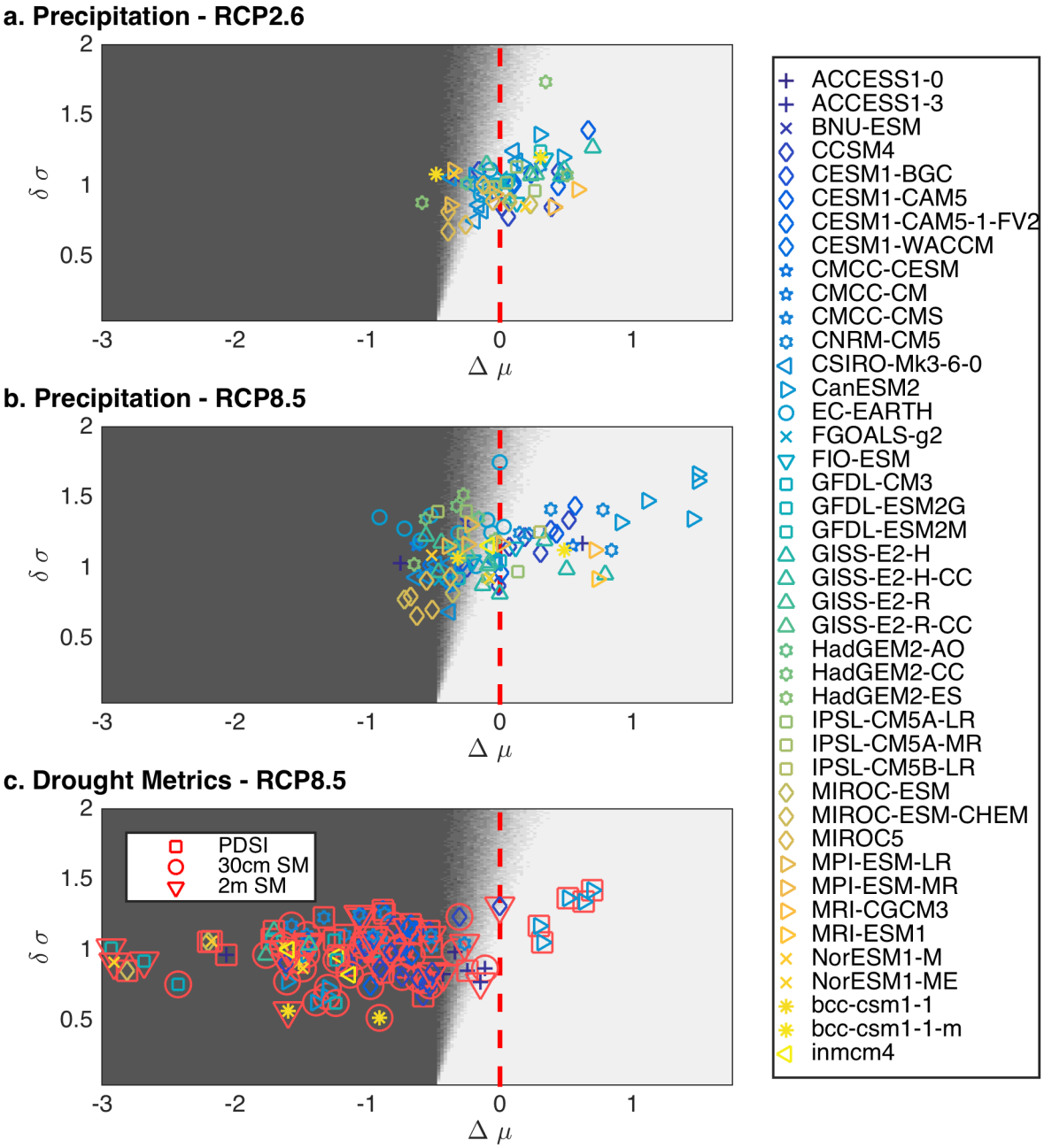
a. Precipitation - RCP2.6
b. Precipitation - RCP8.5
c. Drought Metrics - RCP8.5
δ σ
Δ μ
2
1.5
1
0.5
-3
-2
-1
0
1
PDSI
30cm SM
2m SM
ACCESS1-0
ACCESS1-3
BNU-ESM
CCSM4
CESM1-BGC
CESM1-CAM5
CESM1-CAM5-1-FV2
CESM1-WACCM
CMCC-CESM
CMCC-CM
CMCC-CMS
CNRM-CM5
CSIRO-Mk3-6-0
CanESM2
EC-EARTH
FGOALS-g2
FIO-ESM
GFDL-CM3
GFDL-ESM2G
GFDL-ESM2M
GISS-E2-H
GISS-E2-H-CC
GISS-E2-R
GISS-E2-R-CC
HadGEM2-AO
HadGEM2-CC
HadGEM2-ES
IPSL-CM5A-LR
IPSL-CM5A-MR
IPSL-CM5B-LR
MIROC-ESM
MIROC-ESM-CHEM
MIROC5
MPI-ESM-LR
MPI-ESM-MR
MRI-CGCM3
MRI-ESM1
NorESM1-M
NorESM1-ME
bcc-csm1-1
bcc-csm1-1-m
inmcm4

Figure S1: Joint (2D) PDF of Southwest megadrought risk for a normalized drought indicator time series ($z'(t)$) with various changes in the mean ($\Delta\mu$) and changes in the variance ($\delta\sigma$). In both panels, the gray shading on all panels indicates risk estimated from Monte Carlo simulations of z'_t, expressed as the fraction of realizations with a 35-year megadrought out of all realizations. Symbols on panels (**a.**) and (**b.**) correspond to changes in the mean and variance of *precipitation only* in the CMIP5 models (colored by model according to the legend) for RCP2.6 and 8.5, respectively. Estimates of changes in the mean and variance from a wider range of *drought metrics* in the 17-model subset (employed by *(7)*) are plotted on panel (**c.**). In all calculations, changes in the mean and variance are computed over the period 2051-2100 and compared to 1951-2000.

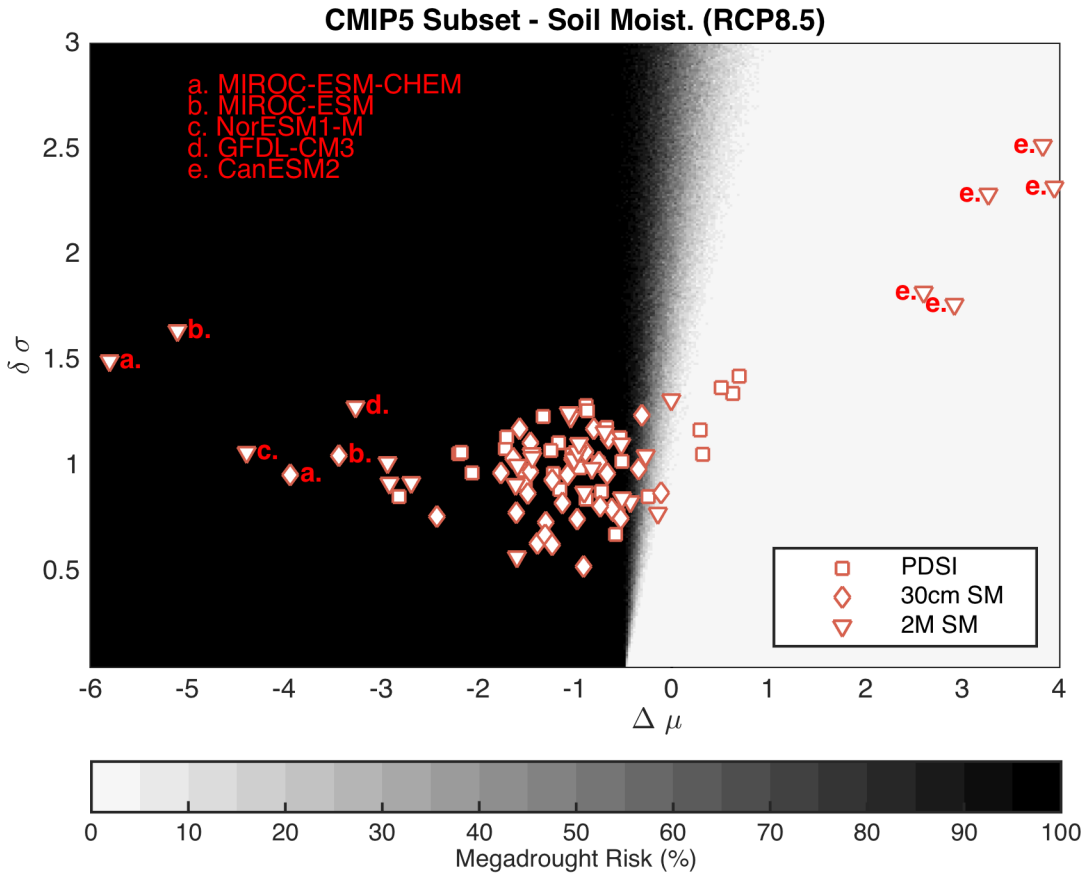

Figure S2: Full range of changes in mean ($\Delta\mu$) and variability ($\delta\sigma$) simulated by CMIP5 model subset. Only the approximate interquartile range is shown for the equivalent plot in Figure 1 of the main text.

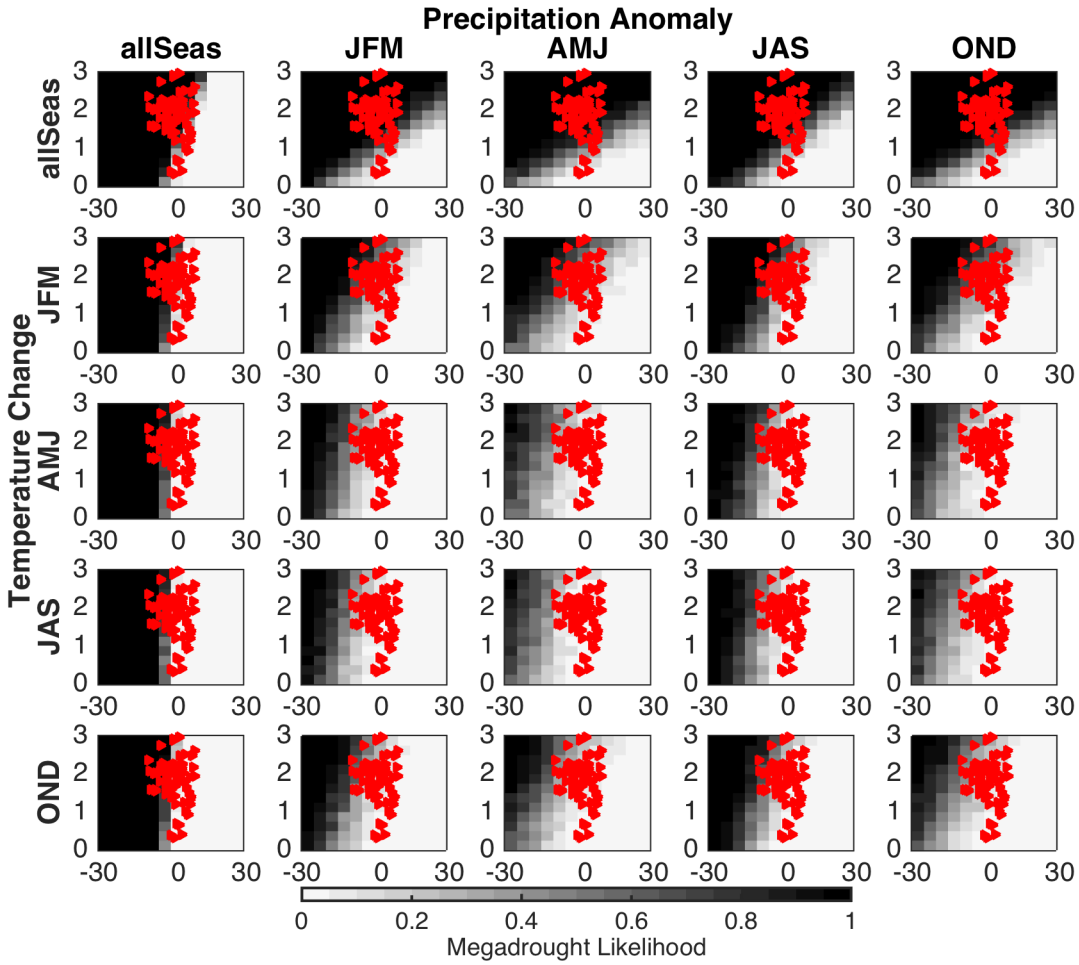

Figure S3: Megadrought PDF for various combinations of seasonal changes. Each panel is megadrought risk in JJA PDSI from a combination of T and P changes during a given season. The upper left corner is the same as Figure 2 of the main text: changes in T and P are applied uniformly over all seasons. Each of the other panels summarizes risks from only introducing changes during a given season. Each column is the PDF resulting from changing precipitation for each of the seasons labeled above that row; each row is the result of changing temperature only during a given season (labeled on the y axis of each row). The magnitudes of the seasonal precipitation or temperature anomalies are given by the x and y axes of each panel, respectively. Temperature changes are only shown up to 3^oC because this range is consistent with the amount of warming seen in the majority of models for the RCP2.6 experiment. Correspondingly, the small red triangles are the T and P results from RCP2.6 experiments (e.g., the same as the triangles in Figure 2 of the main text).

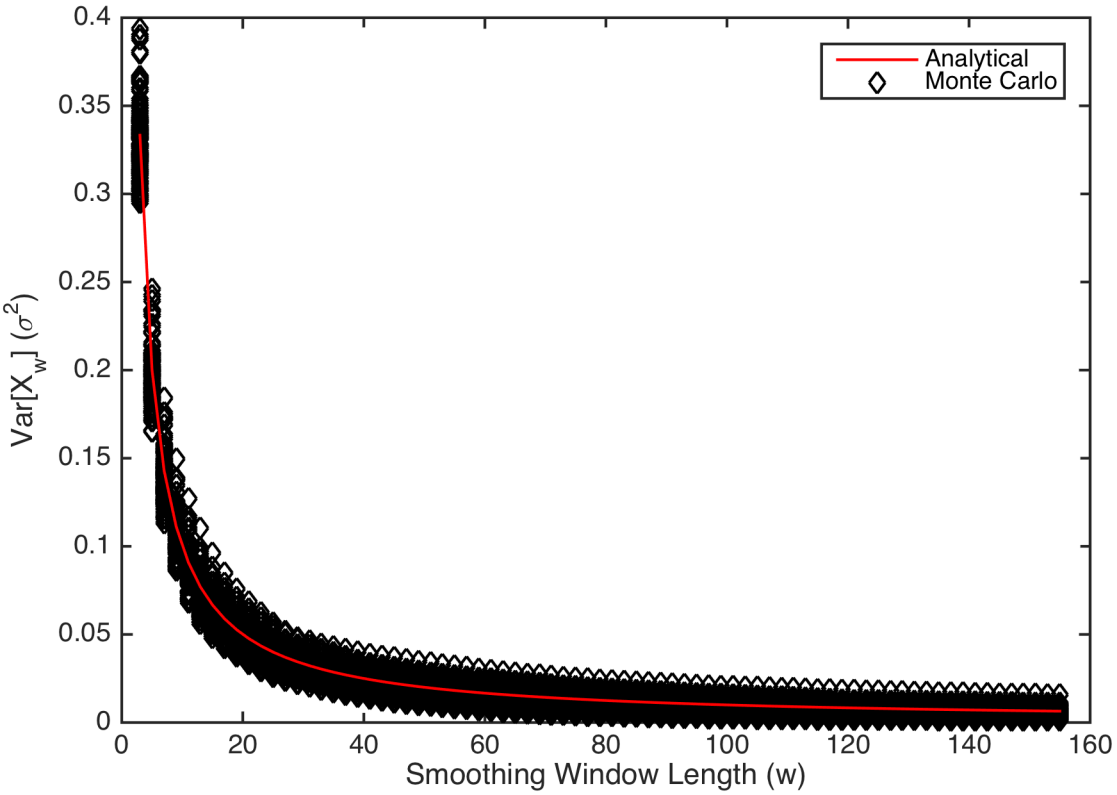

Figure S4: Reduction of variance in smoothed time series (X_w) as a function of smoothing window length (w). The red line shows the reduction in variance predicted by $1/w$, while the diamonds show the range of variances computed from Monte Carlo realizations of X_w for different window lengths.

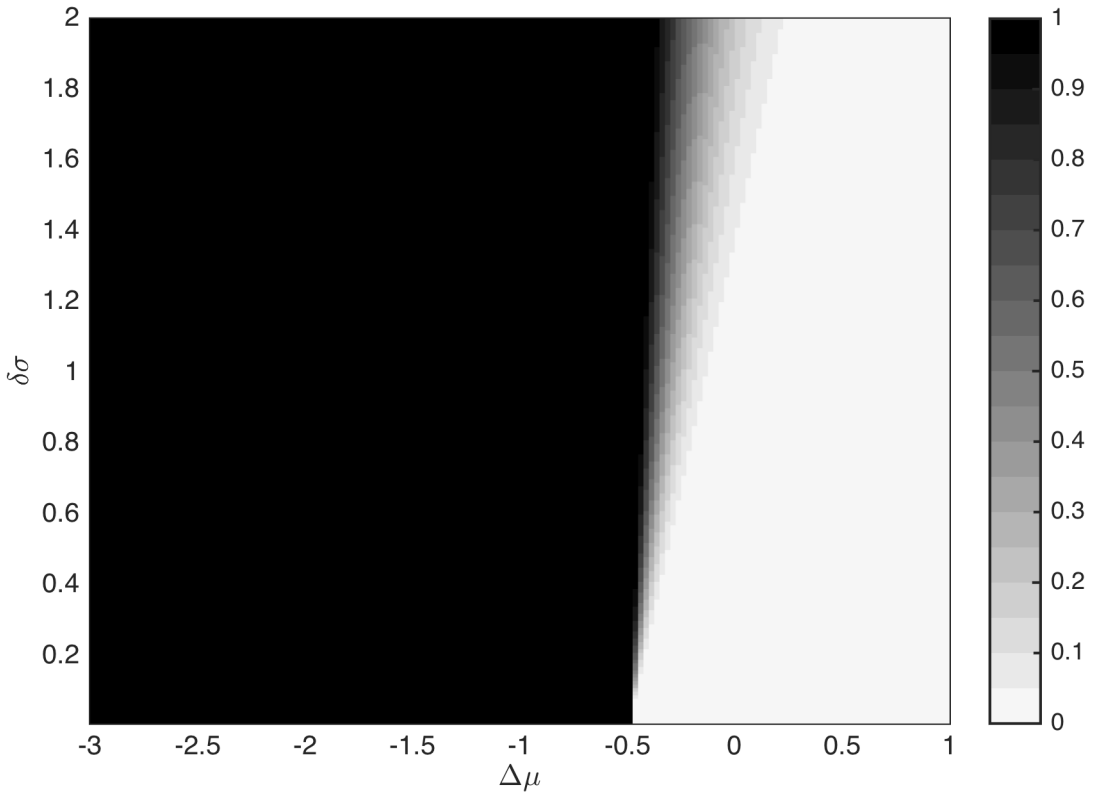

Figure S5: 2D PDF of prolonged drought risk computed from the analytical expression for megadrought probability. Note that here raw probabilities are used instead of percentages as in Figure 1 of the main text.

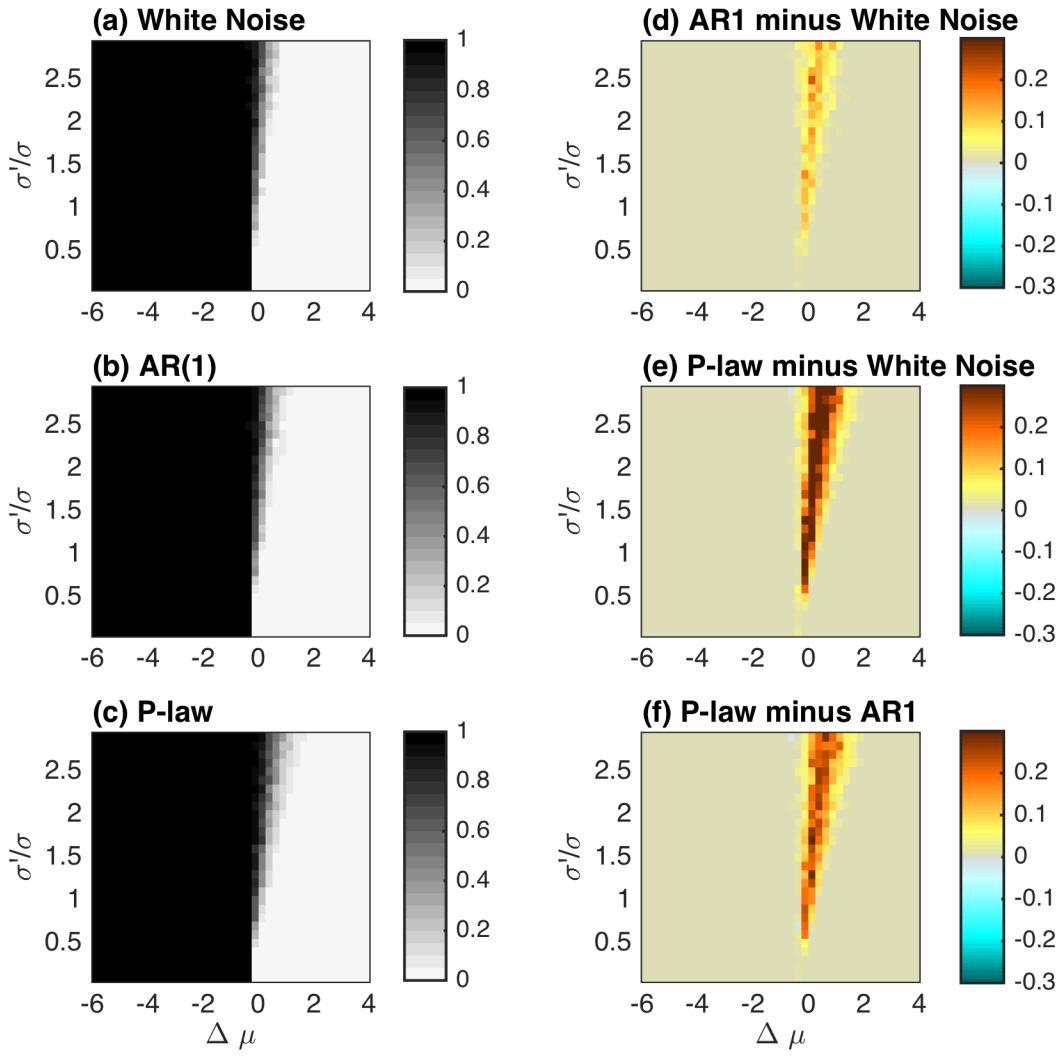

Figure S6: **(Left side)** Megadrought 2D PDF for changes in mean and variance, but for different autocorrelation characteristics of the z-index: **(a)** white noise, as in **Fig. 1** of the main text; **(b)** one-year lag autocorrelation (AR(1)) comparable to observations in the Southwest ($\rho = 0.2$, e-folding time of 7 months); and, **(c)** Power law distribution ($\beta = 0.5$). **(Right side)** Differences in 2D megadrought PDFs between: **(d)** the AR(1) and white noise distributions; **(e)** power-law and white noise; and **(f)** power-law and AR(1). As in Figure S5, the units of these PDFs are probabilities, not percentages as in Figure 1 of the main text.